RESEARCH PAPER

LC–HRMS, Molecular Docking, and ADMET-Based Evaluation of Qurs-E-Ziabetus Khas for Antidiabetic Potential

Kamati Mounika[1], P. Dharani Prasad[1]*

.

[1]*Department of Pharmacology, School of Pharmaceutical Sciences (Erstwhile Sree Vidyaniketan College of Pharmacy), Mohan Babu University, Tirupati 517102, Andra Pradesh, India*

Received: 14th Aug, 2025; Revised: 15th Sep 2025; Accepted: 18th Nov, 2025; Available Online: 1st December, 2025

ABSTRACT

Qurs-e-Ziabetus Khas (QZKH) is an Unani polyherbal-mineral formulation used for the management of diabetes mellitus (Ziabetus Shakri). This study used to analyze its phytochemical, physicochemical, pharmacological, and molecular attributes to scientifically establish its therapeutic effectiveness. Physicochemical and organoleptic tests showed that QZKH tablets are smooth, and compact, with a pH of 6.2 to 6.9, a low moisture content of 4.1%, and no microbiological or heavy metal contamination. This indicates that the product is good quality as well as safe. Phytochemical analysis revealed the presence of flavonoids, alkaloids, tannins, phenolics, and saponins, indicating antioxidant and hypoglycemic effects. Profiling using LC-HRMS found important chemicals such rutin (m/z 683.4), quercetin (m/z 303), procyanidin B2 (m/z 578), and ginsenoside Rb1 (m/z 1123.6), which are known to help with diabetes and have antioxidant properties. ADMET study showed that quercetin, rutin, and procyanidin B2 have good absorption, distribution, and low toxicity profiles. Molecular docking results demonstrated that quercetin showed strong binding affinities with α-glucosidase (−7.8 kcal/mol) and glucokinase (−8.0 kcal/mol); rutin exhibited high affinity toward α-amylase (−5.2 kcal/mol) and DPP-IV (−9.3 kcal/mol); and procyanidin B2 showed significant interactions with α-amylase (−5.1 kcal/mol) and DPP-IV (−9.1 kcal/mol). These strong binding interactions demonstrate that multiple targets are being inhibited in significant enzymes that control glucose levels. The results confirm the traditional Unani statements, confirming QZKH as a scientifically validated, safe, and efficacious antidiabetic formulation with robust multi-mechanistic activity using antioxidant, enzyme-inhibitory, and insulin-sensitizing pathways

Keywords: Qurs-e-Ziabetus Khas; Phytochemical profiling; Computational analysis; LC–HRMS; Diabetes mellitus; Unani medicine.

How to cite this article: Mounika K., Prasad PD. LC–HRMS, Molecular Docking, and ADMET-Based Evaluation of Qurs-e-Ziabetus Khas for Antidiabetic Potential. Int J Drug Deliv Technol. 2026;16(1): 08-33. DOI: 10.25258/ijddt.16.1.2

Source of support: Nil.

Conflict of interest: None

INTRODUCTION

Diabetes mellitus (DM) is a complicated metabolic illness that causes high blood sugar levels gradually because the body doesn't make enough insulin or the insulin doesn't work properly. Recent scientific research shows that DM is not just a disruption of glucose metabolism but a complex metabolic syndrome characterized by oxidative stress, mitochondrial dysfunction, chronic inflammation, and an imbalance of the gut microbiota[1,2,3]. These variables together cause insulin resistance, β-cell death, and metabolic rigidity. The International Diabetes Federation estimates that more than 700 million people will have diabetes, by 2045. This shows the important to find safer, more effective, and less expensive ways to treat it. Current pharmacotherapies, including metformin, sulfonylureas, DPP-IV inhibitors, and SGLT2 inhibitors, effectively lower blood glucose levels. However, their long-term use is frequently constrained by adverse effects, diminished efficacy, and an inability to target the oxidative and inflammatory pathways that contribute to diabetic complications[4,5,6]. Therefore, global study has moved toward looking at traditional healing methods that focus on regulating metabolic balance as an overall plant-based formulations containing many bioactive components.

The Unani system of medicine, a long-standing holistic healing tradition, provides several polyherbal and mineral compositions with established therapeutic efficacy. Historically, Qurs-e-Ziabetus Khas (QZKH) has been administered for Ziabetus Shakri (diabetes mellitus). This well-known technique uses synergistic elements including Tinospora cordifolia (Satt-e-Gilo), Syzygium cumini (Maghz-e-Khasta-e-Jamun), Gymnema sylvestre (Gurmar Booti), Bambusa bambos (Tabasheer), Plantago ovata (Laoob-e-Aspaghol), and Kushta-e-Zamurrud (Emerald calx). These components are said to have a wide range of pharmacological effects, such as helping pancreatic β-cells redevelopment, modulating carbohydrates, controlling lipids, and protecting cells from oxidative damage. Therefore, the formulation is a natural, multi-component way to manage blood sugar and stabilize metabolism[7,8].

Modern pharmacognosy and computational biology provide methodologies to scientifically substantiate traditional formulas. Liquid Chromatography High Resolution Mass Spectrometry (LC–HRMS) and other methods allow to complete profiles of phytochemical

**Author for Correspondence: dharaniprasadp@gmail.com*

ingredients, which helps to find the essential bioactive compounds that are responsible for medicinal effectiveness[9]. While employed with in silico methods like molecular docking and ADMET (Absorption, Distribution, Metabolism, Excretion, and Toxicity) assessments, these methods provide an extensive view of compounds interact with targets, pharmacokinetic behavior, and safety [10,11.] α-amylase, α-glucosidase, Dipeptidyl Peptidase-IV (DPP-IV), and glucokinase are all very important in glucose metabolism. α-Amylase and α-glucosidase help break down complex carbs into monosaccharides that can be absorbed. This affects blood sugar levels after meals. DPP-IV controls incretin hormones like GLP-1, which increases insulin production and glucose tolerance [12,13,14.] Glucokinase, act as a glucose sensor in the liver and pancreas, encouraging glycogen synthesis and maintaining energy balance. Inhibiting or changing these enzymes is a proven way to treat high blood sugar and make insulin work more effectively.

The phytoconstituents found in QZKH, include flavonoids, alkaloids, saponins, phenolics, and glycosides, are renowned for their high antioxidant, hypoglycemic, and enzyme-inhibitory properties. Quercetin, rutin, and procyanidin B2 are examples of compounds that have been demonstrated to prevent α-amylase and α-glucosidase from operating. While ginsenosides and saponins modulate insulin signaling and glucose uptake. These multifunctional attributes provide QZKH a good option for mechanistic validation by combined in silico and in vitro methodologies. The current work seeks to evaluate the bioactive components of QZKH by LC–HRMS profiling, molecular docking, and ADMET analysis, focusing on essential diabetes enzymes—α-amylase, α-glucosidase, DPP-IV, and glucokinase. LC–HRMS identifies phytochemicals at excellent resolution, and molecular docking shows how they bind to and interact with target enzymes. The ADMET study examines the behavior of compounds function in the body, such as their capacity to move through the body and safety standards, to see whether they might be used as drugs. This approach combines old Unani practices with modern molecular research, giving scientific proof that QZKH works to fight diabetes and showing that it might be a safe, multi-faceted therapy for the disease.

MATERIALS AND METHODS

Purchase and Procurement of Qurs-E-Ziabetus Khas

The Unani formulation of QZKH was obtained from a licensed local Unani medicine shop in Hyderabad, Telangana, India. The medication was obtained in its commercially available tablet form, included in manufacturer-labeled packaging to ensure authenticity and traceability (Figure 1). All necessary measures were implemented during purchase to ensure the product was neither expired nor compromised, and the batch number and expiry date were recorded for reference.

Following purchase, the formulation was subjected to organoleptic evaluation and quality verification, including the assessment of physical characteristics such as color, odor, and texture. The material was thereafter preserved in regulated, arid conditions at ambient temperature to avert any deterioration until analysis. The acquired formulation was later used for first phytochemical screening and chromatographic separation of phytoconstituents. The research aims to detect significant secondary metabolites and bioactive chemicals associated with the documented antidiabetic action of the formulation.

Figure 1. The *QZKH* tablet purchased from licensed local Unani medicine outlet in the Hyderabad city, Telangana, India

Sample Preparation

We collected 10 tablets of QZKH and utilized them to prepare the sample (Figure 2). Initially the tablets were checked for uniformity. After this, they were crushed into a fine powder using a clean, dry mortar and pestle in a clean environment. To make sure that the powder was even and to get rid of any large pieces, it was filtered again using a 60-mesh screen. The fine powder that was made was carefully mixed and stored in a glass container that was airtight and amber-colored to keep out moisture, light, and germs. This standardized sample was utilized in a lot of different tests, such as phytochemical screening, microbiological testing, and physicochemical analysis
.

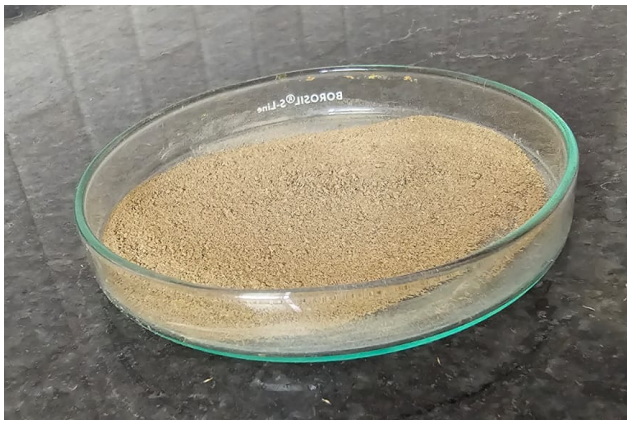

Figure 2. Sample of QZKH

Physicochemical Analysis

The physicochemical analysis of the sample included assessing its sensory, chemical, and compositional attributes to ensure high standards of quality and purity. The color was examined in natural light, and the fragrance and taste were checked by sniffing and tasting immediately. A digital pH meter was used to find out the pH of 1% and 10% water solutions. We separated out the foreign material and counted it as a part of the overall sample. We utilized the loss on drying (LOD) at 105 °C to identify moisture existed in the sample. Also measured the ash values, including total ash, acid-insoluble ash, sulphated ash, and water-soluble ash, to find out how much inorganic material was present. To determine alcohol and water solubility of extract, we used 90% alcohol and chloroform water. Atomic absorption spectrophotometry was used to look at heavy metals such arsenic, cadmium, lead, mercury, zinc, copper, chromium, and manganese after acid digestion with 3 M HNO_3. We were able to measure pesticide residues using gas chromatography with a ^{63}Ni electron capture detector under the ideal conditions. The limits of detection were between 0.1 and 0.5 ppb, and the recovery rates were above 80%. The analysis demonstrated that the material satisfied the standards for physicochemical properties and was ready for further testing[15,16,17].

Preliminary Phytochemical Screening

The phytochemical screening of the raw material shows the existence of many bioactive chemicals. Carbohydrates, monosaccharides, and reducing sugars were verified using Molisch's, Fehling's, Barfoed's, and Benedict's assays. Amino acids and proteins provided good results in Biuret, Ninhydrin, and Millon's test. Oils and fats were identified using saponification, while steroids exhibited positive Salkowski and Liebermann–Burchard responses. Glycosides, including anthraquinone, cardiac, and saponin varieties, were validated by Keller-Killiani, Borntrager's, and foam assays. Flavonoids were identified using lead acetate and Shinoda assays, whereas alkaloids were found using Dragendorff's, Wagner's, Mayer's, and Hager's reagents. Tannins and phenolic compounds yielded good findings in the ferric chloride and lead acetate assays. The results indicate that the sample comprises many secondary metabolites of pharmacological significance[18,19,20.]

Microbial Content and Specific Microorganism Determination

Microbial analysis was conducted to determine total viable counts and identify specific pathogens. One gram of powdered or one milliliter of liquid sample was serially diluted in sterile distilled water and plated on Nutrient, MacConkey, Cetrimide, and Sabouraud dextrose agars using the pour plate method. Plates were incubated at 37 °C for 24 hours for bacteria and 27 °C for 72 hours for fungi. Colony-forming units were then recorded. Enrichment and selective media were used to identify pathogens: E. coli (MacConkey broth), Salmonella (Deoxycholate citrate agar after enrichment), Shigella (Salmonella–Shigella agar, TSI confirmation), P. aeruginosa (Cetrimide agar, oxidase test), and S. aureus (MSA, catalase, and coagulase tests). These procedures provided a comprehensive assessment of microbial safety and quality[21,22,23].

LC-HRMS Analysis

The LC-HRMS investigation used an Accucore C18 column of 150 × 4.6 mm with a particle size of 2.6 µm. The extract was analyzed using both positive and negative electrospray ionization (ESI) techniques to ensure comprehensive metabolite profiling. We used gradient elution to separate the samples by chromatography, and we got mass spectra for the whole m/z range from 150 to 2000. Instrument software was used to collect and evaluate data in order to find the primary ion peaks and their respective retention durations. To identify a compound, we used accurate mass, isotopic distribution, and fragmentation patterns. Then, we used literature and standard mass spectral databases to make a brief record of the compound[9,24,25,26].

ADMET analysis

The ADMET research was conducted to evaluate the pharmacokinetic and toxicity characteristics of the chosen phytoconstituents. Molecular structures were initially depicted using ChemDraw, and their SMILES notations were sourced from PubChem. The compounds were further analyzed with SwissADME to assess properties pertaining to absorption, distribution, metabolism, and excretion, encompassing gastrointestinal absorption, blood-brain barrier permeability, and P-glycoprotein interactions. The toxicological characteristics, encompassing hepatotoxicity, carcinogenicity, and LD_{50}, were assessed using ADMETlab 3.0. Results were evaluated using known drug-likeness criteria, including Lipinski's rule of five, to determine drug-likeness and oral bioavailability. This comprehensive study enabled the prompt detection of potential pharmacological and safety issues[13,27,28].

Molecular Docking

After ADMET studies, Molecular docking was performed to identify antidiabetic efficacy of phytoconstituents in QZKH by targeting four essential enzymes: Alpha-Glucosidase (3WY2), Alpha-Amylase (PDB ID: 3BAX), Glucokinase (1V4S), and Dipeptidyl Peptidase-IV (DPP-IV; 2P8S). The structures of the selected compounds were shown using ChemDraw and generated into 3D conformers

with PubChem. The crystal structures of the target enzymes were obtained from the RCSB Protein Data Bank. Proteins were produced with Discovery Studio by eliminating water molecules and ligands, and adding hydrogen atoms. The grid box was defined around the active site coordinates specific to each enzyme: Alpha-Amylase (X: 7.101571, Y: 32.660071, Z: -7.511786), Alpha-Glucosidase (X: -38.692273, Y: 12.098000, Z: -26.594000), DPP-IV (X: 41.248845, Y: 51.547173, Z: 36.546362), and Glucokinase (X: 40.210304, Y: 15.085435, Z: 61.973217). Ligand files were converted to PDBQT format using PyRx, and molecular docking was executed using AutoDock Vina. Binding affinities were recorded, and interactions were visualized with Discovery Studio[29,30,31,32]. 3D representation for molecular docking of selected compounds with selected enzymes are shown in Figure 3.

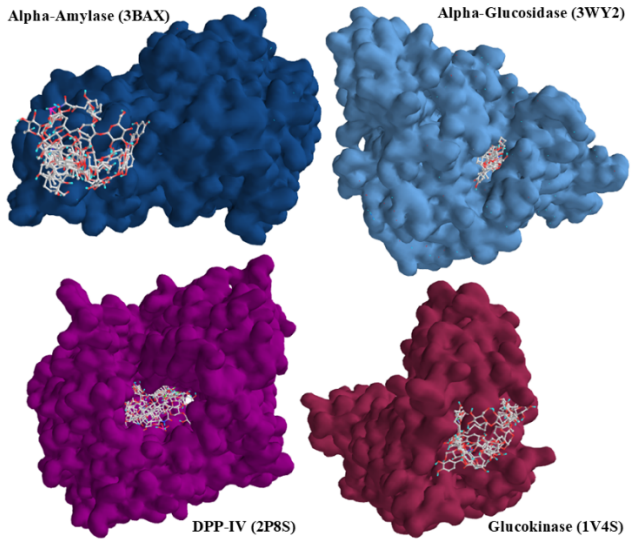

Figure 3. 3D representation for molecular docking of selected compounds with Alpha-Amylase (3BAX), Alpha-Glucosidase (3WY2), Dipeptidyl Peptidase-IV (DPP-IV, 2P8S), and Glucokinase (1V4S).

RESULTS AND DISCUSSION

QZKH: Composition and Pharmacological Profile

QZKH is a conventional Unani herbal-mineral formulation that has been utilized for an extended period to manage diabetes mellitus (Ziabetus Shakri). It enhances pancreatic function, regulates blood glucose levels, accelerates metabolism, and safeguards cells from injury. Each tablet contains Tabasheer (Bambusa bambos, 73.53 mg), a siliceous, cooling demulcent that facilitates tissue healing and glucose utilization; Satt-e-Gilo (Tinospora cordifolia, 73.53 mg), a potent immunomodulatory and hypoglycemic herb that enhances insulin secretion and promotes liver health; and Maghz-e-Khasta-e-Jamun (Syzygium cumini, 29.41 mg), which is rich in jamboline and ellagic acid, thereby inhibiting the conversion of starch to sugar. Gurmar Booti (Gymnema sylvestre, 14.70 mg), referred to as the "sugar destroyer," enhances insulin efficacy and facilitates pancreatic recovery. The mineral component, Kushta-e-Zamurrud (Emerald calx, 29.41 mg), serves as an antioxidant and enhances metabolism. The botanical element, Laoob-e-Aspaghol (Plantago ovata, Q.S.), is a soluble fiber that retards carbohydrate absorption and maintains stable blood glucose levels postprandially. When mixed together, these chemicals collaboratively maintain stable blood glucose levels, enhance metabolic processes, and safeguard against oxidative stress. QZKH is an exceptional polyherbal formulation for the management of diabetes.

Organoleptic and Physicochemical Analysis of Samples

The tablets of QZKH were evaluated for physicochemical and organoleptic characteristics to identify their purity and quality (Figure 4). The tablets were gray, possessed a distinct herbal scent, displayed a slight astringent taste, and featured a hard, smooth, and compact texture, signifying strong mechanical integrity. Physicochemical analysis revealed pH values of 6.9 for a 1% solution and 6.2 for a 10% solution, indicating a nearly neutral nature suitable for oral administration. The drying loss was 4.1%, signifying suitable moisture content, but total ash (8.9%), acid-insoluble ash (1.4%), water-soluble ash (5.9%), and sulphated ash (1.3%) exhibited minimal inorganic impurities. The extractive values were 18.5% (alcohol-soluble) and 24.56% (water-soluble), signifying the presence of bioactive chemicals in both polar and non-polar fractions. Analyses for heavy metals and pesticide residues produced negative findings, affirming the formulation's safety and compliance with quality standards.

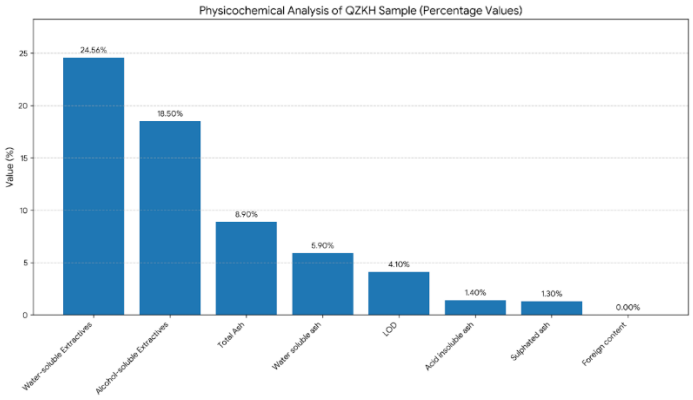

Figure 4. The physicochemical analysis of QZKH Sample

Microbial Content Determination

The microbial content determination of the QZKH tablets provided the complete absence of pathogenic microorganisms, including *Salmonella spp.*, *Escherichia coli*, *Staphylococcus aureus*, *Pseudomonas aeruginosa*, and *Shigella spp.* This indicates that the formulation is microbiologically safe and contamination free that could pose health risks. The sterility of the sample reflects effective control during manufacturing and storage, aligning with pharmacopeial standards and ensuring the product's quality and safety for consumer use.

Preliminary Phytochemical Screening of Sample

The initial phytochemical analysis of QZKH tablets (Figure 5) demonstrated a diverse array of bioactive compounds, underscoring the formulation's pharmacological potential. Carbohydrates, reducing sugars, and monosaccharides were identified in minimal quantities, although proteins and

amino acids had a low presence. Fats and oils were detected in moderate amounts, indicating lipid-soluble phytoconstituents that facilitate absorption. Steroids and cardiac glycosides were detected at trace amounts, whereas anthraquinone glycosides were undetectable, signifying the absence of purgative effects. Moderate levels of saponin glycosides indicate potential metabolic and immunomodulatory advantages. The significant abundance of alkaloids, phenolic compounds, tannins, and flavonoids suggests robust antioxidant, antibacterial, and anti-diabetic properties, hence reinforcing the therapeutic effectiveness of QZKH in the management of diabetes and associated metabolic diseases.

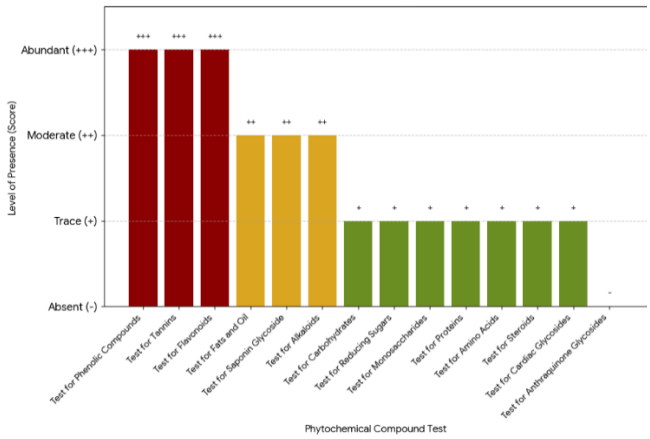

Figure 5. The results of preliminary phytochemical screening of QZKH tablets

LC-HRMS Analysis

The LC-HRMS analysis of QZKH was conducted in both ESI+ and ESI– ionization modes to identify a diverse array of phytoconstituents with variable polarities and molecular weights (Table 1 and Figure 6). The total ion chromatograms (TIC) in both ionization modalities exhibited separate but complimentary peak patterns. Early eluting peaks (<5 min) were associated with polar phenolic compounds, whereas mid-retention peaks (5–10 min) were mostly comprised of flavonoid glycosides and polyphenolic dimers. Late-eluting peaks (>10 min) signified the presence of substantial hydrophobic compounds, including triterpenoid saponins, ginsenosides, and lipid derivatives, aligning with secondary metabolites characteristic of medicinal plants utilized in traditional Unani formulations. High-resolution mass spectrometry data, corroborated by accurate mass comparisons, isotopic patterns, and literature references, facilitated the provisional characterisation of many bioactive phytoconstituents. Prominent identified ions comprised m/z 683.4, 847.5, 1123.6, 1256.7, and 1531.7 (ESI+), as well as m/z 681.6, 665.5, 959.6, 1400.4, and 1547.5 (ESI–). The elevated mass-to-charge ratios indicate the prevalence of glycosylated molecules. Significant peaks with retention durations of 6.06 and 6.30 minutes with m/z values of 683.4 and 845.4 were tentatively identified as rutin, a flavonoid glycoside often documented in antidiabetic medications. Signals at m/z 847.5 and 765.5 between 10 and 14 minutes are indicative of triterpenoid saponins, aligning with their amphiphilic properties and protracted elution characteristics.

A prominent molecular ion at m/z 1123.6 seen at 9.74 minutes corresponds to ginsenoside Rb1, a pharmacologically significant derivative of ginseng, recognized for its antihyperglycemic and adaptogenic properties. Furthermore, high mass ions above 1200 m/z during 14–17 minutes corresponded to Lipid A derivatives, perhaps signifying the presence of biomolecules implicated in immunomodulation. Additional phenolic components, including quercetin (m/z 303) and procyanidin B2 (m/z 578), were identified, corroborating the formulation's significant antioxidant capacity. Proanthocyanidins, including procyanidin B2, are recognized for their ability to inhibit α-amylase and α-glucosidase, hence corroborating the traditional application of QZKH in type 2 diabetes management.

Table 1. Tentative identification of phytoconstituents in Qurs-E-Ziabetus Khas (QZKH) based on LC–HRMS analysis

Compound	Class/Type	Justification (m/z match, RT, etc.)	Potential Use/Application
Rutin	Flavonoid glycoside	Matches m/z 610–630, retention time 6–7 min	Antioxidant, anti-inflammatory
Saponin	Triterpenoid glycoside	Matches m/z 847–870, recurring pattern	Immunostimulant, antifungal
Ginsenoside Rb1	Glycosylated triterpene	m/z >1000, RT 10–12 min	Adaptogenic, neuroprotective
Lipid A derivative (Lipid A-disaccharide-1-phosphate)	Lipid	m/z >1200, broad RT 14–17 min	Endotoxin component, signaling
Quercetin	Flavonoid aglycone	m/z 303, detected in both modes	Antioxidant, cancer research
Procyanidin B2	Polyphenol dimer	m/z 578	Cardiovascular health, food antioxidant

The variety of discovered chemicals indicates that QZKH is phytochemically abundant and may possess multifunctional pharmacological properties. Numerous identified substances, such as rutin, quercetin,

procyanidins, and ginsenosides, are shown to exhibit inhibitory effects against α-glucosidase and α-amylase, enhance insulin sensitivity, and safeguard pancreatic β-cells. These data empirically substantiate the conventional Unani use of QZKH for glycemic regulation. Furthermore, the identification of saponins and polyphenolic antioxidants substantiates the formulation's efficacy in mitigating oxidative stress, a significant pathogenic factor in diabetes mellitus and its consequences.

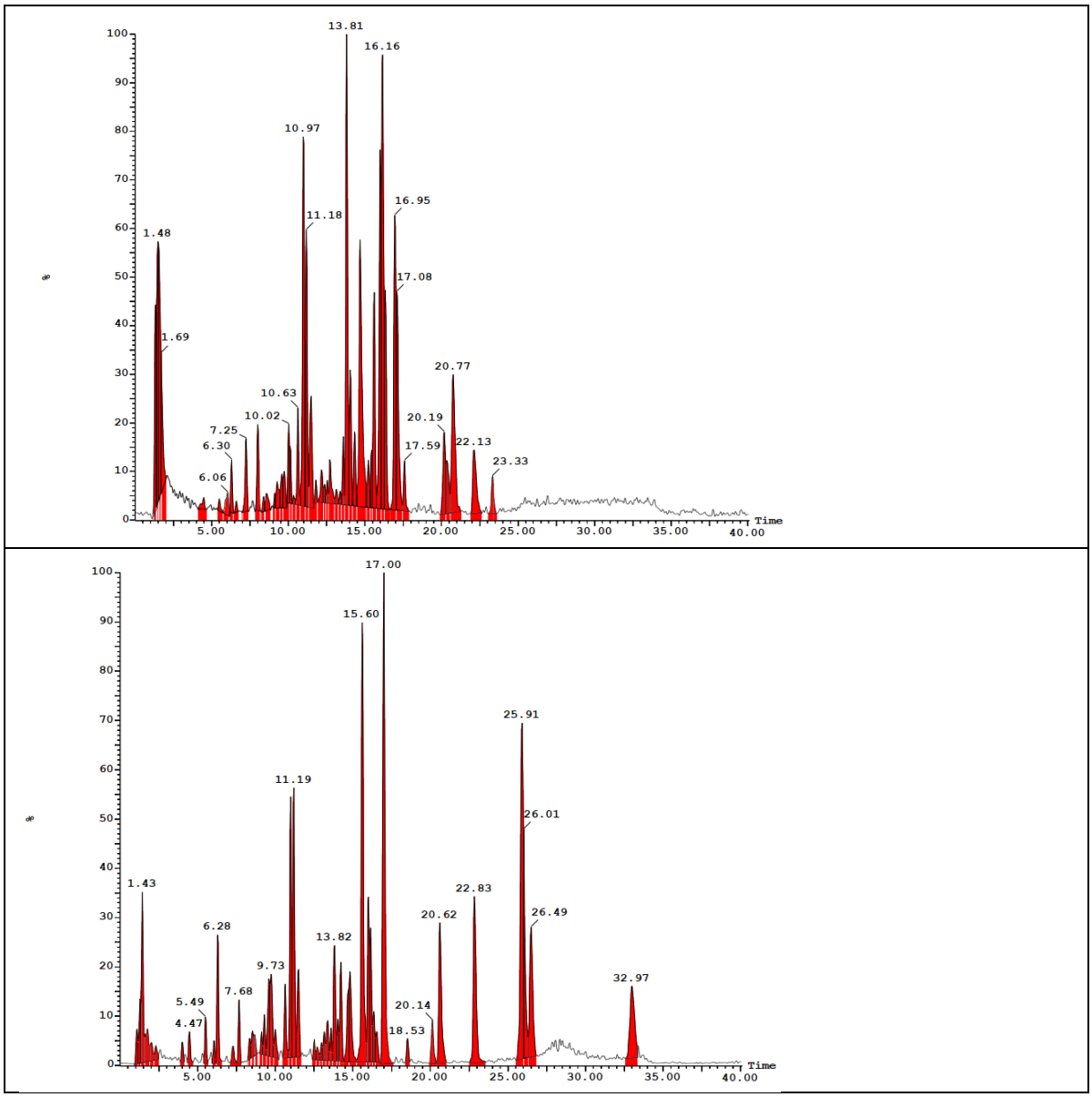

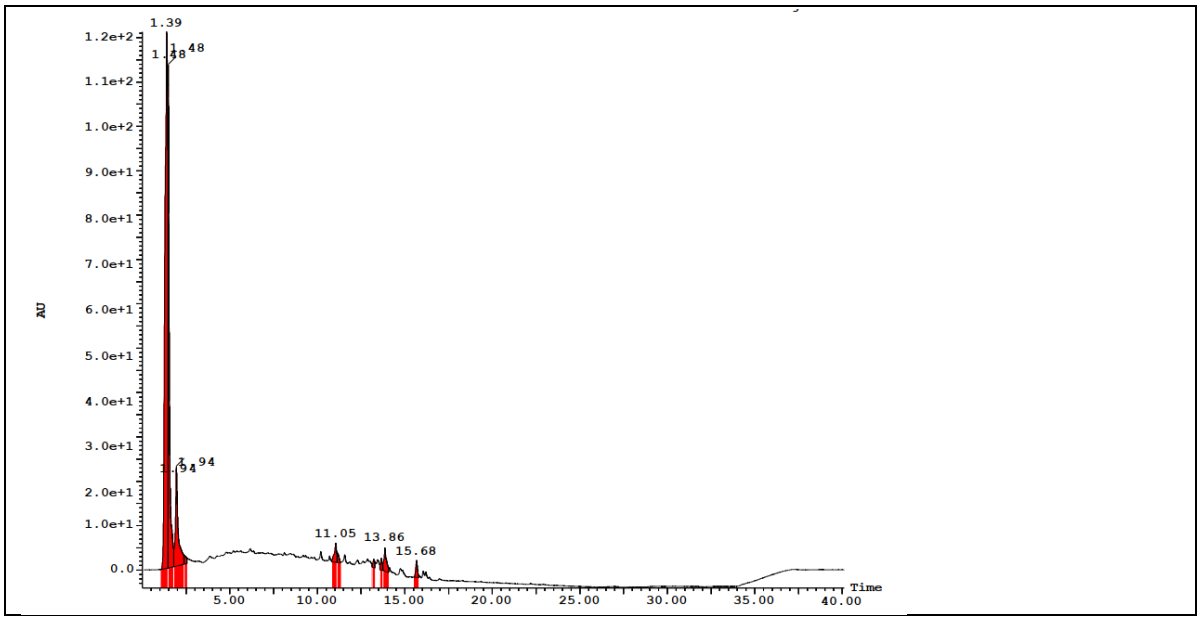

Figure 6. LC-HRMS graph of QZKH extract

ADMET Analysis

The physicochemical study of the identified phytoconstituents from Qurs-E-Ziabetus Khas shown significant discrepancies in alpha-amylase (3BAX), alpha-glucosidase (3WY2), DPP-IV (1V4S), and glucokinase (2P8S). Native ligands (NLs) demonstrated comparatively lower molecular weights (MW 180–419 Da), reduced total polar surface area (TPSA: 59.97–119.25 Å²), and fewer hydrogen bond donors/acceptors, suggesting advantageous drug-likeness (Table 2). Conversely, components such as Ginsenoside Rb1, Lipid A-disaccharide-1-phosphate, and Saponin exhibited significantly large molecular weights (>1000 Da), increased topological polar surface areas (>300 Å²), and a substantial number of rotatable bonds and hydrogen donors, potentially inhibiting membrane permeability and oral bioavailability. Procyanidin B2, Quercetin, and Rutin exhibited intermediate characteristics, possessing moderate molecular weight and balanced polarity, rendering them more analogous to native ligands. Specifically, Quercetin and Procyanidin B2 demonstrated physicochemical properties akin to NLs, indicating an enhanced possibility for enzyme interaction while preserving drug-like attributes. These results inform the choice of lead compounds for further biological assessment.

Table 2. Physicochemical properties of selected derivatives with four native ligands

Compounds	MW	Volume	Dense	nHA	nHD	nRot	nRing	TPSA	logS	logP
NL-3BAX	221.09	199.4695	1.10839	7	5	3	1	119.25	0.274001	-1.80564
NL-3WY2	180.06	156.5173	1.150416	6	5	1	1	110.38	0.322626	-2.20092
NL-1V4S	349.05	310.7988	1.123074	6	3	5	3	85.83	-4.01038	2.352379
NL-2P8S	419.15	363.8652	1.151938	5	2	3	4	59.97	-3.83598	2.310712
Ginsenoside Rb1	1108.6	1073.627	1.032575	23	15	16	8	377.29	-4.40642	1.234332
Lipid A-disaccharide-1-phosphate	1324.89	1374.65	0.963802	22	11	62	2	346.86	-0.49343	8.91904
Procyanidin B2	578.14	549.9425	1.051274	12	10	3	6	220.76	-3.31173	1.149859

Quercetin	302.04	282.7668	1.068159	7	5	1	3	131.36	-3.72159	1.447712
Rutin	610.15	552.3177	1.104708	16	10	6	5	269.43	-2.39666	0.986122
Saponin	1222.6	1152.302	1.061006	27	15	14	11	422.05	-2.69315	-0.73569

The drug-likeness profile of the identified compounds was evaluated using four native ligands—NL-3BAX, NL-3WY2, NL-1V4S, and NL-2P8S (Table 3). Among the chosen compounds, Quercetin demonstrated a QED of 0.434, surpassing NL-3BAX (0.337) and NL-3WY2 (0.29), while residing between NL-2P8S (0.6) and NL-1V4S (0.707), signifying moderate drug-likeness. Furthermore, Quercetin did not contravene the Lipinski, Pfizer, GSK, or Golden Triangle rules, akin to the majority of native ligands, but it did breach the Chelator Rule, a transgression also observed in some ligands such as NL-3WY2. Conversely, Ginsenoside Rb1 and Saponin had markedly low QED scores (0.058), substantially inferior to all native ligands, indicating inadequate drug-likeness. Both molecules contravened the Lipinski, GSK, and Golden Triangle criteria, which native ligands often adhered to. This underscores their inadequate oral bioavailability and worse pharmacokinetics relative to native ligands. Procyanidin B2, although possessing a respectable NP Score (1.929), exhibited a low QED (0.159) and contravened Lipinski, GSK, Golden Triangle, and Chelator Rules, signifying a diminished drug-likeness profile relative to all native ligands. Rutin had a comparable pattern, characterized by a low QED of 0.14 and several rule infractions. Lipid A-disaccharide-1-phosphate exhibited little drug-like characteristics (QED 0.015) and violated many criteria, placing it well below native ligands for drug-likeness.

Table 3. Drug-likeness properties of selected derivatives with four native ligands

Compounds	**QED**	**NP Score**	**Lipinski Rule**	**Pfizer Rule**	**GSKRule**	**GoldenTriangle**	**Chelator Rule**
NL-3BAX	0.337	2.019	0	0	0	0	0
NL-3WY2	0.29	2.627	0	0	0	1	0
NL-1V4S	0.707	-2.4	0	0	0	0	0
NL-2P8S	0.6	-0.766	0	0	1	0	0
Ginsenoside Rb1	0.058	1.987	1	0	1	1	0
Lipid A-disaccharide-1-phosphate	0.015	0.66	1	0	1	1	0
Procyanidin B2	0.159	1.929	1	0	1	1	1
Quercetin	0.434	1.701	0	0	0	0	1
Rutin	0.14	2.015	1	0	1	1	1
Saponin	0.058	2.021	1	0	1	1	0

The absorption characteristics of the identified compounds exhibited differing pharmacokinetic potential relative to the native ligands (Table 4). Ginsenoside Rb1 and Saponin demonstrated suboptimal Caco-2 permeability (−6.86 and −6.89), inferior to NL-3BAX and NL-3WY2, signifying decreased intestinal absorption. Notwithstanding this, Saponin exhibited exceptional oral bioavailability (F50%: 0.9998), surpassing all native ligands. Procyanidin B2 had the lowest Caco-2 permeability (−7.22) and exceedingly poor human intestinal absorption (0.00036), indicating suboptimal absorption relative to all native ligands. Quercetin exhibited moderate permeability and favorable oral absorption (F50%: 0.998), surpassing NL-1V4S (0.666) and being equivalent to NL-3WY2 (0.816). Rutin and Lipid A-disaccharide-1-phosphate had superior projected bioavailability within the F20–F50% range, exceeding that of native ligands like NL-2P8S, which displayed little absorption (F50%: 0.0004). Lipid A-disaccharide-1-phosphate, although being a potent P-glycoprotein substrate akin to NL-3BAX, has elevated absorption metrics. Rutin, Quercetin, and Lipid A-disaccharide-1-phosphate shown enhanced absorption properties relative to the majority of native ligands.

Table 4. Absorption parameter of selected compounds with four native ligands

Compounds	Caco-2 Permeability	MDCK Permeability	Pgp-inhibitor	Pgp-substrate	HIA	F20%	F30%	F50%
NL-3BAX	-6.37263	-5.12885	0.002236	0.880931	0.94665	0.180412	0.97263	0.795713
NL-3WY2	-6.40469	-4.93176	0.000546	0.515461	0.964196	0.228636	0.956875	0.816721
NL-1V4S	-4.77376	-4.66453	0.042789	0.000318	0.50995	0.391325	0.961656	0.666846
NL-2P8S	-4.98787	-4.7128	0.933971	0.066047	2.46E-05	9.74E-05	0.000683	0.000405
Ginsenoside Rb1	-6.8638	-4.95157	2.59E-05	0.517312	0.989354	0.185309	0.999868	0.998844
Lipid A-disaccharide-1-phosphate	-6.10515	-5.30345	1.28E-08	0.979923	0.968914	0.999915	1	1
Procyanidin B2	-7.22239	-4.86908	1.49E-06	0.084725	0.000367	0.997977	0.999981	0.999995
Quercetin	-6.17681	-4.92272	0.027569	0.030731	0.133589	0.5038	0.99108	0.998593
Rutin	-6.54652	-5.02701	6.22E-08	0.699256	0.639735	0.772111	0.999751	0.999936
Saponin	-6.89354	-5.1059	9.11E-09	0.835719	0.619858	0.174493	0.999043	0.999837

The distribution and metabolism results indicate varied pharmacokinetic profiles among the selected drugs and native ligands (Table 5). Quercetin and Lipid A-disaccharide-1-phosphate exhibited exceptionally strong plasma protein binding (PPB% >98%), surpassing all native ligands except NL-1V4S (94%), which suggests a decreased quantity of free drug in plasma. Lipid A-disaccharide-1-phosphate had the largest volume of distribution (VD: 1.36), indicating significant tissue penetration, in contrast to Quercetin (VD: −0.87), which is predominantly plasma-restricted. Quercetin, Rutin, and Saponin exhibited minimal penetration of the BBB, in stark contrast to NL-3WY2, which demonstrated a high BBB score of 0.76. Quercetin inhibited many CYP enzymes in metabolism, including CYP1A2, CYP3A4, and CYP2D6, akin to NL-1V4S, indicating a possibility of drug–drug interactions. Procyanidin B2 and Rutin exhibited selective inhibition of cytochrome P450 enzymes, although with poor substrate affinity. Ginsenoside Rb1 and Saponin demonstrated little CYP inhibition or substrate activity, suggesting low metabolic liability. Quercetin and Lipid A-disaccharide-1-phosphate exhibited intricate but possibly significant distribution and metabolic characteristics compared to native ligands

.

Table 5. Distribution and metabolism parameter of selected molecules with four native ligands

Compounds	Distribution				Metabolism									
					CYP1A2		CYP2C19		CYP2C9		CYP2D6		CYP3A4	
	PPB%	VD	BBB	Fu	Inhibitor	Substrate	Inhibitor	Substrate	Inhibitor	Substrate	Inhibitor	Substrate	Inhibitor	Substrate
NL-3BAX	13.95247	-0.52554	0.438822	88.68793	0.004324	0.000106	0.001866	3.30E-05	0.235022	0.000868	0.00161	0.001371	0.000138	0.000132
NL-3WY2	28.27579	-0.49815	0.760185	74.52975	0.014336	0.000784	5.14E-05	3.44E-05	0.000683	0.059492	0.00302	4.77E-05	0.000189	0.000344
NL-1V4S	94.09742	-0.14663	0.025883	5.173788	0.173242	0.000167	0.99957	0.00416	0.999426	0.899177	0.005836	0.000734	0.995015	0.000129
NL-2P8S	78.91359	0.586892	0.390839	16.74723	0.005937	0.999993	5.65E-06	0.854881	8.47E-05	2.41E-05	0.005479	0.000422	3.17E-05	0.001574

Ginsenoside Rb1	61.80754	-0.36051	0.003427	22.51776	4.19E-22	1.40E-08	2.97E-14	0.004699	1.32E-07	1.24E-10	2.98E-14	1.44E-16	5.95E-09	6.83E-05
Lipid A-disaccharide-1-phosphate	99.00459	1.363994	9.29E-12	1.155782	3.28E-08	3.93E-28	0.577727	5.61E-13	2.83E-05	0.999805	0.017296	0.181481	0.362418	1.47E-15
Procyanidin B2	90.33684	0.269515	0.00494	17.46273	4.84E-11	0.999999	0.000129	0.022383	1.74E-07	0.637389	3.82E-15	3.39E-13	3.79E-08	2.60E-06
Quercetin	98.65997	-0.87913	0.000445	1.131221	0.998312	0.38429	0.005855	4.87E-05	0.432249	0.029644	0.00018	0.978297	0.936699	1.34E-06
Rutin	85.0054	-0.05883	3.59E-05	14.65911	0.0001	0.00364	1.44E-07	1.07E-06	1.85E-06	7.47E-05	2.26E-06	1.48E-07	0.029205	2.29E-09
Saponin	54.54499	-0.3726	1.65E-05	32.97135	9.16E-21	9.00E-05	2.13E-16	0.006025	2.24E-08	2.86E-07	1.03E-13	2.31E-16	1.59E-06	0.887254

The excretion and toxicity profiles of the selected compounds differed markedly from those of the native ligands (Table 6). Quercetin and Procyanidin B2 exhibited elevated plasma clearance rates (8.28 and 8.93 mL/min/kg, respectively), signifying more rapid removal compared to any native ligand, particularly NL-1V4S and NL-2P8S, which had longer half-lives but reduced clearance rates. Lipid A-disaccharide-1-phosphate had the longest half-life (5.33 h), indicating prolonged systemic presence, but Rutin and Saponin both displayed extended half-lives (>3.9 h), surpassing those of the majority of native ligands. Regarding toxicity, Quercetin exhibited comparatively low human hepatotoxicity (H-HT: 0.33) and moderate respiratory toxicity (0.67), superior to NL-1V4S (H-HT: 0.93, Respiratory: 0.94). Procyanidin B2 and Rutin had less skin sensitivity and carcinogenic potential, rendering them safer than NL-1V4S, which had a high projected carcinogenicity of 0.70. Ginsenoside Rb1 and Saponin exhibited little oral toxicity and no dermal or ocular irritation. Rutin, Quercetin, and Lipid A-disaccharide-1-phosphate exhibited advantageous excretion and low to moderate toxicity profiles compared to native ligands.

Table 6. Excretion and Toxicity parameters of selected compounds with four native ligands

Compounds	**Excretion**		**Toxicity**									
	CL-plasma	**T1/2**	**H-HT**	**DILI**	**Ames Toxicity**	**Rat Oral Acute Toxicity**	**FDAMDD**	**Skin Sensitization**	**Carcinogenicity**	**Eye Corrosion**	**Eye Irritation**	**Respiratory Toxicity**
NL-3BAX	1.772639	2.328189	0.55989	0.495928	0.796281	0.046798	0.018939	0.957543	0.173344	0.000456	0.75277	0.060898
NL-3WY2	1.63333	2.385782	0.409855	0.387216	0.754114	0.039753	0.01464	0.951218	0.077268	0.028417	0.953642	0.032698
NL-1V4S	3.70086	0.877237	0.933633	0.999995	0.894723	0.219646	0.120982	0.841064	0.707188	2.65E-07	0.492436	0.945703
NL-2P8S	3.917	1.229357	0.990451	0.44045	0.359812	0.996691	0.989483	0.8946	0.15544	0.000536	0.047347	0.999947
Ginsenoside Rb1	-0.35695	3.721897	0.687761	0.804434	0.988105	0.000122	5.28E-05	1	0.019511	9.48E-12	2.76E-05	3.79E-05

Lipid A-disaccharide-1-phosphate	2.536052	5.332315	0.785021	0.062583	3.47E-05	0.000104	0.791345	1	0.014105	0.00028	0.769297	0.999837
Procyanidin B2	8.926722	3.979776	0.842384	0.7412	0.710891	0.744531	0.962248	0.999985	0.023725	3.41E-06	0.899264	0.954631
Quercetin	8.288988	1.58575	0.337382	0.782596	0.586042	0.479917	0.788757	0.896924	0.600177	0.603284	0.998417	0.673657
Rutin	1.610724	4.616005	0.406325	0.936922	0.756376	0	0.137174	0.997444	0.046632	3.59E-05	0.904546	0.030272
Saponin	-0.68619	3.937869	0.785881	0.774382	0.987314	0.000224	0.001287	1	0.013417	1.23E-13	4.53E-06	9.17E-05

The environmental toxicity profile of the identified compounds reveals differing ecological safety in relation to the native ligands (Table 7). Quercetin, Procyanidin B2, and Rutin exhibited elevated LC_{50} values for fathead minnow (FM) and Daphnia magna (DM), ranging from 4.1 to 4.9, indicating minimal aquatic toxicity and rendering them safer than NL-3BAX and NL-3WY2, which presented considerably lower LC_{50} values (FM: approximately 2.3 and 1.6; DM: approximately 2.9 and 2.3, respectively). Lipid A-disaccharide-1-phosphate had the greatest IGC_{50} (5.96), signifying little cytotoxicity to green algae, however demonstrated a low LC_{50}FM (0.6), showing selective aquatic toxicity. Regarding bioaccumulation, NL-2P8S had the greatest BCF (1.98), signifying a greater potential for environmental persistence. The majority of chosen chemicals, such as Quercetin (1.21) and Procyanidin B2 (1.17), had moderate BCF values, which were inferior than NL-2P8S, indicating a decreased risk of bioaccumulation. Rutin, Saponin, and Quercetin demonstrated superior environmental safety, surpassing the majority of native ligands in aquatic toxicity metrics.

Table 7. Environmental toxicity profile of selected molecules with four native ligands

Compounds	BCF	IGC50	LC50FM	LC50DM
NL-3BAX	0.091368	1.715961	2.298723	2.971279
NL-3WY2	0.196614	1.420954	1.681152	2.344653
NL-1V4S	0.50029	3.159616	3.858534	4.481158
NL-2P8S	1.984816	3.500606	4.099818	4.846382
Ginsenoside Rb1	1.294527	3.43607	3.830685	4.679278
Lipid A-disaccharide-1-phosphate	-0.78587	5.967977	0.600727	7.745741
Procyanidin B2	1.177655	3.630484	4.187311	4.706862
Quercetin	1.210035	3.758566	4.112	4.485008
Rutin	0.533413	3.180953	3.927314	4.680011
Saponin	0.488305	3.304285	3.780041	4.908842

Table 8. ADMET radar of all selected compounds with four native ligands

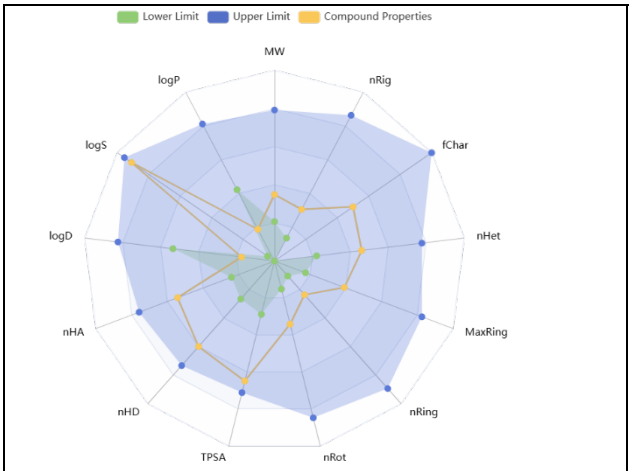 NL-3BAX	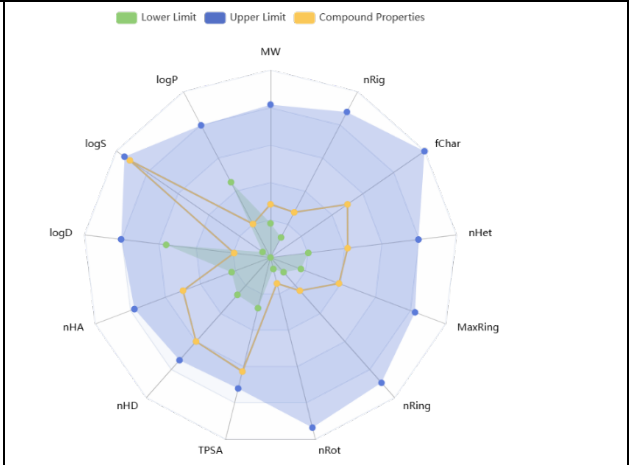 NL-3WY2
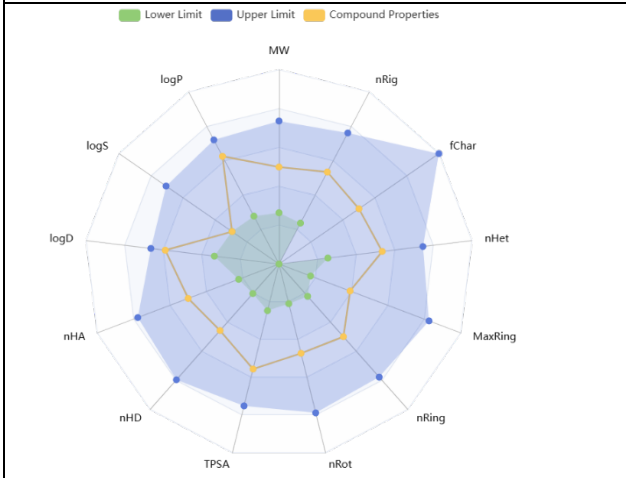 NL-1V4S	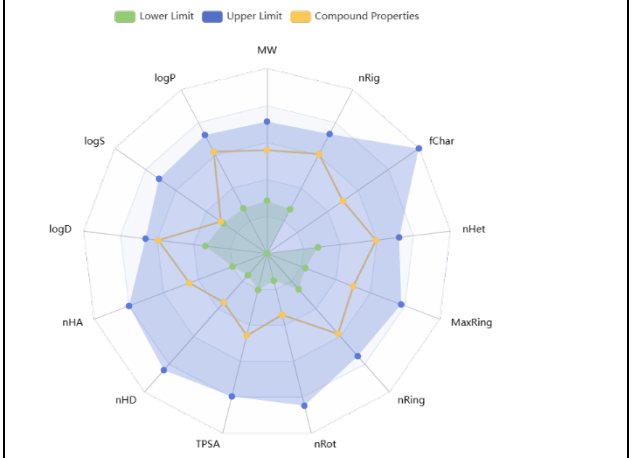 NL-2P8S
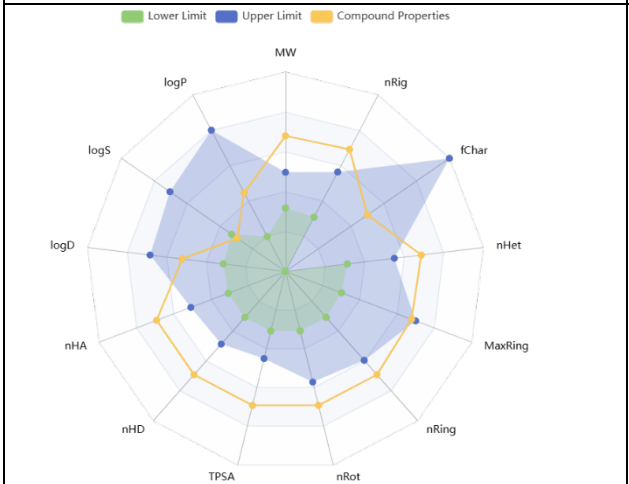 Ginsenoside Rb1	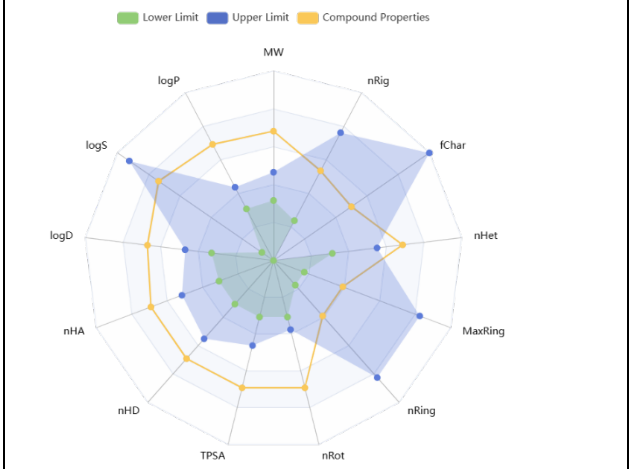 Lipid A-disaccharide-1-phosphate

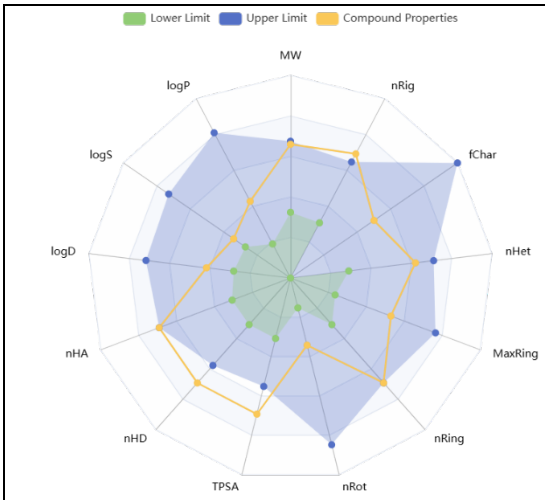

Procyanidin B2

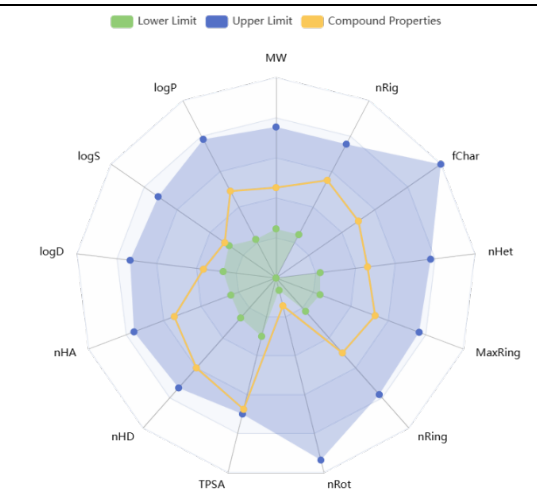

Quercetin

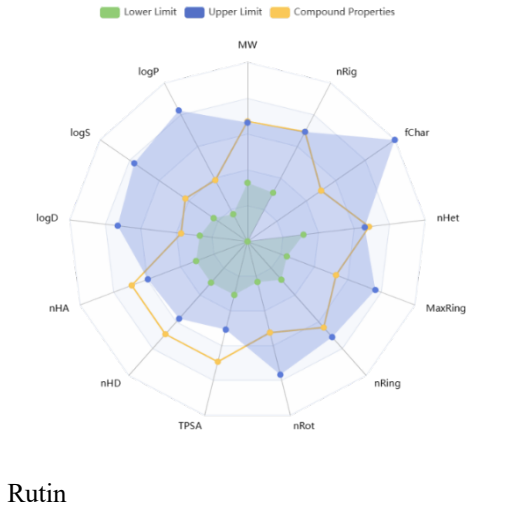

Rutin

Saponin

Molecular Docking

This study systematically assessed the bioactive phytoconstituents of QZKH for their antidiabetic efficacy via molecular docking against four pivotal enzymes implicated in glucose metabolism and regulation: Alpha-Amylase (3BAX), Alpha-Glucosidase (3WY2), Dipeptidyl Peptidase-IV (DPP-IV, 2P8S), and Glucokinase (1V4S) (Table 9). Molecular docking simulations were conducted to evaluate the binding affinities, interaction patterns, and structural compatibility of chosen elements with the active sites of these enzymes. Native ligands co-crystallized with each protein were similarly docked and examined for comparability. The docking outcomes were assessed according to binding energy (kcal/mol), the quantity and kind of interactions (hydrogen bonds, electrostatic, hydrophobic), and the amino acid residues implicated. This comparative research identifies phytochemicals that may serve as effective enzyme inhibitors or modulators, exhibiting superior or equivalent performance to native ligands, thereby offering mechanistic insight into the antidiabetic activity of QZKH. Figure 7 illustrates both 2D and 3D representations of all powerful derivatives, alongside all enzymes with their corresponding native ligands.

Alpha-Amylase (3BAX)

Native ligand of alpha-amylase (3BAX) exhibited a binding affinity of -4.0 kcal/mol, establishing numerous hydrogen bonds with GLU493 and participating in electrostatic (pi-cation) and hydrophobic (pi-alkyl) interactions with LYS457. Rutin demonstrated the highest binding affinity among the phytochemicals, measuring -5.2 kcal/mol. It established large hydrogen bonding connections with GLU493, LYS457, and GLY460, in addition to notable pi-cation and amide-pi stacking interactions, indicating increased stability inside the active site. Procyanidin B2 (-5.1 kcal/mol) surpassed the native ligand by establishing hydrogen bonds with THR448 and LYS466, as well as a pi-alkyl interaction with LEU496. Saponin (-4.9 kcal/mol) and Quercetin (-5.0 kcal/mol) exhibited many hydrogen bonds and significant hydrophobic interactions, suggesting superior binding affinity compared to the native ligand. Lipid A-disaccharide-1-phosphate and Ginsenoside Rb1, although establishing several hydrogen bonds, had lower binding scores (-2.6 and -3.7 kcal/mol, respectively), while maintaining advantageous interactions with critical residues

such as THR448 and ASN461. Their elevated molecular weight and polar surface areas may diminish binding affinity due to steric hindrance. These data indicate that certain phytoconstituents of QZKH may function as superior alpha-amylase inhibitors compared to the native ligand.

Alpha-Glucosidase (3WY2)

The native ligand of alpha-glucosidase (3WY2) had a binding affinity of -5.7 kcal/mol, engaging in hydrogen bonding with GLY228, ASP202, and GLU271, and forming hydrophobic interactions with PHE166. Rutin achieved a binding score of -5.7 kcal/mol, establishing several hydrogen bonds and generating electrostatic and hydrophobic interactions, including pi-anion, pi-cation, and pi-pi stacking with residues such as ARG400, ASP333, and PHE397, indicating a robust binding conformation. Quercetin had the greatest affinity of -7.8 kcal/mol, establishing robust hydrogen bonds and electrostatic contacts with ARG400 and ASP333, as well as maintaining hydrophobic connections, suggesting its potential as a formidable alpha-glucosidase inhibitor. In contrast, several molecules such as Ginsenoside Rb1 (+6.9 kcal/mol) and Lipid A-disaccharide-1-phosphate (+4.5 kcal/mol) had positive docking scores, signifying unfavorable or weak binding affinities. Saponin (+18.0 kcal/mol) had a significantly elevated positive energy, indicating its potential ineffectiveness in inhibiting alpha-glucosidase in its present state. Consequently, molecules such as Quercetin, Rutin, and Procyanidin B2 are distinguished as more effective binders than the native ligand.

DPP-IV (2P8S)

The native ligand for DPP-IV (2P8S) exhibited a robust binding affinity of -9.9 kcal/mol via numerous hydrogen bonds with GLU205 and ARG358, in addition to halogen, pi-sigma, and pi-pi stacking interactions. Among the phytoconstituents, Rutin (-9.3 kcal/mol) and Saponin (-9.6 kcal/mol) exhibited binding affinities comparable to those of the native ligand. Rutin demonstrated a varied array of interactions, including hydrogen bonding, pi-donor, pi-anion, and electrostatic contacts with critical residues such as SER630, TYR662, and GLU205, indicating a robust mimicking of the native ligand's interaction profile. Procyanidin B2 (-9.1 kcal/mol) and Ginsenoside Rb1 (-8.9 kcal/mol) exhibited advantageous affinities and established stable hydrogen bonds with essential residues like GLU205 and SER630. Quercetin (-7.7 kcal/mol) exhibited a somewhat reduced affinity while preserving significant interactions. Conversely, Lipid A-disaccharide-1-phosphate (-6.3 kcal/mol) exhibited a moderate affinity and a less robust interaction pattern. Numerous components, including Rutin, Saponin, and Procyanidin B2, closely resemble or even equal the binding capability of the native ligand, indicating their potential for DPP-IV inhibition.

Glucokinase (1V4S)

The native ligand of glucokinase (1V4S) exhibited a binding affinity of -8.5 kcal/mol, interacting with residues including ARG63, LEU451, and THR65 via hydrogen bonding and hydrophobic interactions. Among the evaluated chemicals, Quercetin exhibited a remarkable affinity of -8.0 kcal/mol, characterized by substantial interactions, including hydrogen bonds with ARG63 and TYR215, as well as hydrophobic interactions with MET210 and TYR214. Procyanidin B2 had a favorable affinity (-6.5 kcal/mol), interacting with ARG250 and GLU67 through hydrogen bonds and establishing pi-alkyl interactions with ARG63. Rutin (-7.5 kcal/mol) and Saponin (-4.4 kcal/mol) had relatively lesser affinities; nonetheless, Rutin established several interactions with residues including TYR214, ARG250, and MET235. Ginsenoside Rb1 demonstrated a binding score of -0.8 kcal/mol, indicating poor or non-productive binding, maybe attributable to steric obstruction or inadequate fit inside the binding pocket. Lipid A-disaccharide-1-phosphate (-3.1 kcal/mol) exhibited poor binding as well. These findings underscore Quercetin and Procyanidin B2 as potential glucokinase modulators with greater affinity than the endogenous ligand.

Table 9. Binding interactions of selected derivatives with Alpha-Amylase (3BAX), Alpha-Glucosidase (3WY2), Dipeptidyl Peptidase-IV (DPP-IV, 2P8S), and Glucokinase (1V4S).

Amino acid residues	Bond Length	Bond Type	Bond Category	Ligand Energy (Kcal/mol)	Binding Affinity
Alpha-Amylase (PDB ID: 3BAX)					
NL-3BAX					
GLU493	2.0672	Hydrogen Bond	Conventional Hydrogen Bond	506.96	-4
GLU493	2.46832				
GLU493	2.44672				
LYS457	4.37265	Electrostatic	Pi-Cation		
LYS457	3.92727	Hydrophobic	Pi-Alkyl		
Lipid A-disaccharide-1-phosphate					
THR448	2.70835	Hydrogen Bond	Conventional Hydrogen Bond	767.09	-2.6
LEU496	2.27346				
CYS462	2.28293				

ASN461	2.92801				
ASN461	2.31343				
LYS466	2.43145				
LYS466	2.97263				
LYS466	2.7071				
Ginsenoside_Rb1					
GLY460	2.00419	Hydrogen Bond	Conventional Hydrogen Bond	862.48	-3.7
LYS466	2.1306				
LYS466	3.06541				
ASN461	3.13628		Carbon Hydrogen Bond		
LEU496	4.56509	Hydrophobic	Alkyl		
LEU496	4.03637				
LEU496	5.42139				
TYR468	5.02857		Pi-Alkyl		
Procyanidin_B2					
THR448	2.12175	Hydrogen Bond	Conventional Hydrogen Bond	499.63	-5.1
LYS466	2.32881				
LEU496	5.08555	Hydrophobic	Pi-Alkyl		
Quercetin					
ASP456	2.1128	Hydrogen Bond	Conventional Hydrogen Bond	181.05	-5
LYS35	4.12558	Electrostatic	Pi-Cation		
ILE458	3.73961	Hydrophobic	Pi-Sigma		
LYS457	4.60837		Pi-Alkyl		
Rutin					
LYS457	2.52285	Hydrogen Bond	Conventional Hydrogen Bond	1639.89	-5.2
GLU493	2.15831				
GLU493	2.81369				
GLY460	2.25993				
LEU496	2.30555				
LYS457	3.66361	Electrostatic	Pi-Cation		
ASN459	3.98915	Hydrophobic	Amide-Pi Stacked		
LYS457	4.72952		Pi-Alkyl		
LYS457	3.92003				
Saponin					
ASN459	1.93407	Hydrogen Bond	Conventional Hydrogen Bond	1050.38	-4.9
ASN459	2.40474				
LEU496	2.16803				
LYS457	2.71028				
ASN461	2.15713				
LYS495	2.33991				
ASN459	3.3181		Carbon Hydrogen Bond		
LEU496	3.78249				
LEU496	4.92484	Hydrophobic	Alkyl		
LEU496	4.92475				
Alpha-Glucosidase (3WY2)					
NL-3WY2					

GLY228	2.23161	Hydrogen Bond	Conventional Hydrogen Bond	447.08	-5.7
ASP202	2.68212				
GLU271	2.56886				
GLU271	2.64405				
PHE166	4.84804	Hydrophobic	Pi-Pi T-shaped		
Lipid A-disaccharide-1-phosphate					
HIS105	2.98558	Hydrogen Bond	Conventional Hydrogen Bond	767.09	4.5
ASP333	2.81658				
ILE272	2.41549				
LEU227	2.67299				
TYR65	2.93614				
ARG200	1.99074				
ARG400	2.23413				
ASP62	2.49289		Carbon Hydrogen Bond		
PRO230	2.62375				
ARG400	2.61372				
PHE77	3.48258	Hydrophobic	Pi-Sigma		
PRO18	2.68893		Alkyl		
ARG19	4.50277				
LEU227	3.50333				
PRO277	3.02081				
VAL335	4.99669				
ARG400	4.30599				
PHE397	5.15741		Pi-Alkyl		
Ginsenoside_Rb1					
HIS105	2.72622	Hydrogen Bond	Conventional Hydrogen Bond	862.48	6.9
ASP333	2.00592				
GLU271	2.59511				
ALA229	2.97897				
GLU231	1.57903				
ASP62	2.43959		Carbon Hydrogen Bond		
GLY228	3.40016				
MET302	3.07243	Other	Sulfur-X		
VAL334	4.74285	Hydrophobic	Alkyl		
ARG400	4.99607				
PRO230	4.22227				
ARG400	4.9283				
ILE146	3.94857				
ALA229	4.2306				
ILE146	4.06211				
PRO230	4.89674				
VAL334	5.39025				
ARG400	4.46554				
ARG400	5.13563				
PHE147	5.47643		Pi-Alkyl		
PHE166	4.82695				

PHE206	4.95563				
TYR235	4.88595				
TYR235	4.54677				
PHE297	5.33094				
TYR389	4.73611				
TYR389	4.15137				
PHE397	4.27739				
PHE397	4.51382				
Procyanidin_B2					
TYR389	2.19961	Hydrogen Bond	Conventional Hydrogen Bond	499.63	2.1
ASP333	2.16554				
TYR389	3.0452				
TYR235	2.65252				
VAL334	3.69179		Carbon Hydrogen Bond		
GLU271	3.45843	Electrostatic	Pi-Anion		
ILE146	3.24014	Hydrophobic	Pi-Sigma		
GLY228	2.97303	Other	Pi-Lone Pair		
TYR389	5.24802	Hydrophobic	Pi-Pi T-shaped		
PHE397	4.79843				
ALA229	4.49064		Pi-Alkyl		
PRO230	4.68414				
Quercetin					
ARG400	2.26084	Hydrogen Bond	Conventional Hydrogen Bond	181.05	-7.8
ARG400	2.76776		Carbon Hydrogen Bond		
ASP333	4.90593	Electrostatic	Pi-Anion		
ASP333	4.33563				
PRO230	5.02259	Hydrophobic	Pi-Alkyl		
VAL334	5.37963				
Rutin					
GLY399	2.20521	Hydrogen Bond	Conventional Hydrogen Bond	1639.89	-5.7
ASP62	2.24338				
GLY228	2.73132				
GLY228	2.93009				
ASP333	3.3369		Carbon Hydrogen Bond		
PRO230	3.65871				
ARG400	3.06228				
ARG400	3.68403	Electrostatic	Pi-Cation		
ASP333	3.82176		Pi-Anion		
PHE166	3.3369	Hydrogen Bond	Pi-Donor Hydrogen Bond		
TYR65	3.53564	Hydrophobic	Pi-Sigma		
VAL335	3.24411				
PHE397	4.82933		Pi-Pi T-shaped		
TYR65	5.73047				
ALA229	5.38607		Pi-Alkyl		
PRO230	4.61304				
PRO230	4.81694				

ARG400	5.309				
HIS332	4.37225				
Saponin					
LEU300	2.10549	Hydrogen Bond	Conventional Hydrogen Bond	1050.38	18
ASP62	1.73802				
ASP62	1.86504				
ASP62	2.45933				
ASN205	2.72955				
ILE272	1.56087				
GLY228	2.59224				
GLY273	2.04168				
TYR235	2.44625				
GLN170	2.54293				
ASP333	3.64581		Carbon Hydrogen Bond		
TYR65	2.49411	Other	Pi-Lone Pair		
MET302	4.45691	Hydrophobic	Alkyl		
MET302	4.7469				
ALA229	4.35207				
PRO230	5.22925				
VAL334	4.32702				
VAL334	4.88775				
VAL335	5.09292				
ALA229	4.00745				
PRO230	4.53799				
VAL334	5.0941				
PHE297	5.35361		Pi-Alkyl		
PHE297	4.88496				
PHE297	4.24602				
PHE297	5.31408				
TYR389	4.77581				
TYR389	5.41837				
PHE397	4.8705				
PHE397	5.10762				
Dipeptidyl Peptidase-IV (DPP-IV; 2P8S)					
NL-2P8S					
GLU205	2.25174	Hydrogen Bond	Conventional Hydrogen Bond	460.23	-9.9
ARG358	3.43518	Hydrogen Bond;Halogen	Conventional Hydrogen Bond;Halogen (Fluorine)		
ARG358	3.24231				
SER630	3.11827				
GLU205	3.61476	Hydrogen Bond	Carbon Hydrogen Bond		
TYR547	3.04914				
ARG358	3.39057				
SER630	3.45107	Halogen	Halogen (Fluorine)		
SER209	3.44072	Hydrogen Bond	Pi-Donor Hydrogen Bond		
TYR662	3.256				
PHE357	3.8145	Hydrophobic	Pi-Sigma		

TYR662	5.02115		Pi-Pi Stacked		
Lipid A-disaccharide-1-phosphate					
ASP556	5.17999	Electrostatic	Attractive Charge	767.09	-6.3
SER577	2.76862	Hydrogen Bond	Conventional Hydrogen Bond		
GLN553	2.18808				
GLN527	3.23265				
ASN562	3.38788				
TYR585	3.27553				
PHE357	3.82632	Hydrophobic	Pi-Sigma		
VAL656	4.33657		Alkyl		
PHE357	4.67827		Pi-Alkyl		
TYR547	5.04214				
TRP629	4.33797				
TYR631	5.11664				
TRP659	5.34724				
HIS748	4.84421				
TYR752	5.13599				
Ginsenoside_Rb1					
GLU205	2.02711	Hydrogen Bond	Conventional Hydrogen Bond	862.48	-8.9
GLU205	2.19692				
GLU206	2.53136				
TYR666	2.2784				
SER630	2.60007				
SER630	2.45732				
TYR752	2.20476				
HIS740	1.77988				
ARG125	2.87091				
SER209	2.94256				
SER209	2.86439				
TYR547	3.25989				
TYR662	3.15111				
TYR666	3.6398	Hydrophobic	Pi-Sigma		
LYS554	4.9878		Alkyl		
LYS554	4.94547				
PHE357	5.14707		Pi-Alkyl		
PHE357 -	5.37876				
TYR547	5.16418				
TYR547	4.23072				
TYR547	4.71901				
TYR547	4.69147				
TYR547	4.42666				
Procyanidin_B2					
CYS551	2.14932	Hydrogen Bond	Conventional Hydrogen Bond	499.63	-9.1
TYR585	2.83949				
GLN553	2.84005				
SER209	3.89809		Pi-Donor Hydrogen Bond		

PHE357	3.82023	Hydrophobic	Pi-Pi Stacked		
ARG356	4.62877		Pi-Alkyl		
Quercetin					
HIS740	2.58311	Hydrogen Bond	Conventional Hydrogen Bond	181.05	-7.7
GLU206	2.38025				
TYR547	2.79836				
TYR662	3.62623		Pi-Donor Hydrogen Bond		
PHE357	4.87403	Hydrophobic	Pi-Pi Stacked		
TYR666	5.72156				
PHE357	4.14665				
TYR662	5.38623				
TYR666	4.81996		Pi-Pi T-shaped		
Rutin					
CYS551	3.01429	Hydrogen Bond	Conventional Hydrogen Bond	1639.89	-9.3
SER630	2.51414				
SER209	2.93146				
GLU206	1.97848				
TYR662	2.46301				
TYR662	2.28672				
SER630	3.21985				
ARG669:	3.35853				
ARG125	3.81685	Electrostatic	Pi-Cation		
GLU205	4.61917		Pi-Anion		
TRP629	2.63736	Hydrogen Bond	Pi-Donor Hydrogen Bond		
TYR547	4.57935	Hydrophobic	Pi-Pi Stacked		
TYR547	4.15965				
PHE357	4.18475				
PHE357	4.56656		Pi-Alkyl		
Saponin					
GLU361	1.90018	Hydrogen Bond	Conventional Hydrogen Bond	1050.38	-9.6
GLU206	2.2795				
GLU206	2.63754				
SER209	2.81997				
SER209	2.84662				
TYR585	3.17722				
ILE405	3.31145		Carbon Hydrogen Bond		
GLU205	3.70551				
PHE357	3.6271	Hydrophobic	Pi-Sigma		
LYS554	5.22434		Alkyl		
PHE357	5.47817		Pi-Alkyl		
TYR547	4.78332				
TYR547	4.31844				
TYR547	3.63836				
TRP629	4.87112				
Glucokinase (1V4S)					
NL-1V4S					

ARG63	2.36716	Hydrogen Bond	Conventional Hydrogen Bond	661.43	-8.5
LEU451	2.83513				
LEU451	2.70475				
THR65	2.26193				
ARG63	2.91034		Pi-Donor Hydrogen Bond		
ILE211	3.60155	Hydrophobic	Pi-Sigma		
MET235	3.88922	Other	Pi-Sulfur		
VAL62	5.16322	Hydrophobic	Pi-Alkyl		
ARG63	5.07984				
PRO66	5.33695				
ILE159	4.81518				
VAL455	5.40417				
ALA456	4.78409				
MET210	4.9715				
Lipid A-disaccharide-1-phosphate					
GLU221	2.01431	Hydrogen Bond	Conventional Hydrogen Bond	767.09	-3.1
ARG63	2.51369				
GLN98	1.95788				
THR65	2.67539				
THR65	2.96905				
TYR215	1.87726				
ARG250	2.97849				
HIS218	3.19053		Carbon Hydrogen Bond		
TYR214	3.1479	Hydrophobic	Pi-Sigma		
ARG63	3.67959		Alkyl		
MET238	4.80819				
PRO66	4.72919				
VAL455	4.91638				
LYS459	4.41434				
Ginsenoside_Rb1					
SER64	1.97647	Hydrogen Bond	Conventional Hydrogen Bond	862.48	-0.8
PRO66	1.82922				
GLU67	3.08546				
TYR214	2.52021				
LYS459	2.43648				
PRO66	3.16725		Carbon Hydrogen Bond		
HIS218	3.7165				
ILE159	4.68099	Hydrophobic	Alkyl		
ILE211	4.99784				
ARG63	4.13417				
PRO66	3.81613				
VAL452	4.58423				
VAL455	3.49902				
ALA456	3.58583				
ILE159	4.30637				
ILE159	4.01476				

ALA456	3.18518				
ILE211	4.99434				
VAL455	4.27541				
VAL455	4.78429				
VAL62	4.84156				
VAL62	4.13107				
VAL452	5.32743				
VAL452	3.58788				
VAL455	5.17872				
VAL455	4.7165				
ALA456	4.48773				
ALA456	4.57207				
TYR215	5.05546		Pi-Alkyl		
TYR215	5.23643				
Procyanidin_B2					
ARG250	2.48517	Hydrogen Bond	Conventional Hydrogen Bond	499.63	-6.5
THR65	2.66826				
GLU67	2.14853				
SER64	2.63122				
ARG63	5.13104	Hydrophobic	Pi-Alkyl		
Quercetin					
LEU451	2.43584	Hydrogen Bond	Conventional Hydrogen Bond	181.05	-8
ARG63	2.45108				
TYR215	2.04098				
VAL62	3.69909	Hydrophobic	Pi-Sigma		
ILE211	3.45241				
MET210	5.8502	Other	Pi-Sulfur		
TYR214	4.16576	Hydrophobic	Pi-Pi Stacked		
PRO66	5.24887		Pi-Alkyl		
ILE211	5.43378				
VAL452	4.65105				
VAL455	4.45671				
MET235	4.74044				
Rutin					
CYS220	1.94296	Hydrogen Bond	Conventional Hydrogen Bond	1639.89	-7.5
SER64	2.30959				
SER64	3.04344				
ARG397	2.79462				
ARG250	4.31216	Electrostatic	Pi-Cation		
ARG250	4.08015	Hydrogen Bond;Electrostatic	Pi-Cation;Pi-Donor Hydrogen Bond		
GLU221	3.80832	Electrostatic	Pi-Anion		
TYR214	2.26912	Hydrogen Bond	Pi-Donor Hydrogen Bond		
TYR214	4.94394	Hydrophobic	Pi-Pi T-shaped		
TYR214	5.449				
VAL62	4.5589		Alkyl		

ILE211	4.74468				
VAL452	4.21313				
MET235	4.87772		Pi-Alkyl		
ILE211	4.94149				
Saponin					
SER64	2.57481	Hydrogen Bond	Conventional Hydrogen Bond	1050.38	-4.4
THR65	2.28922				
THR65	2.39645				
ARG63	2.19036				
GLU67	3.47924		Carbon Hydrogen Bond		
PRO66	3.82127	Hydrophobic	Alkyl		
ARG63	4.60022				
PRO66	4.06838				
ARG63	4.97147				
PRO66	5.05422				
PRO66	4.12073				
PRO66	5.11637				
LYS459	5.24973				
LYS459	4.90702				

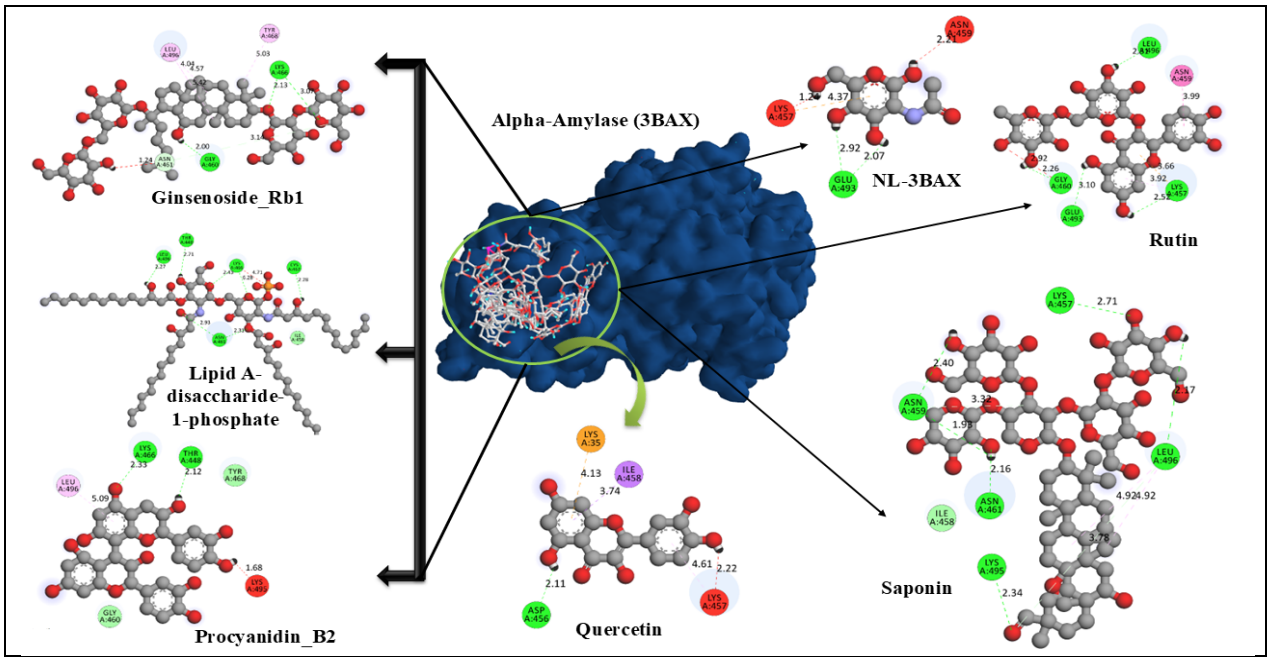

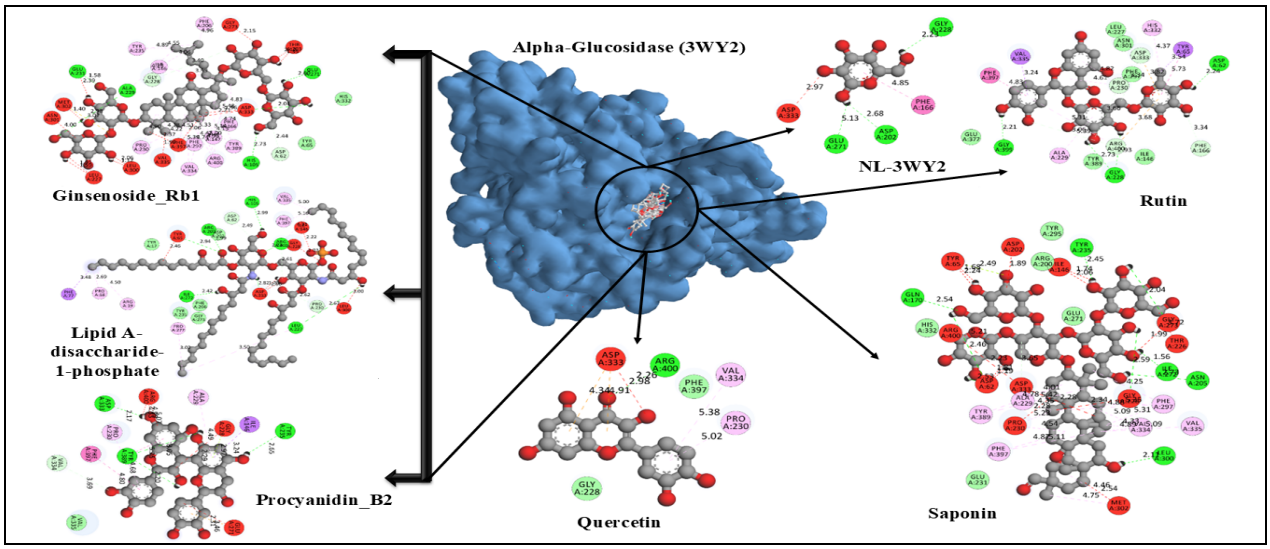

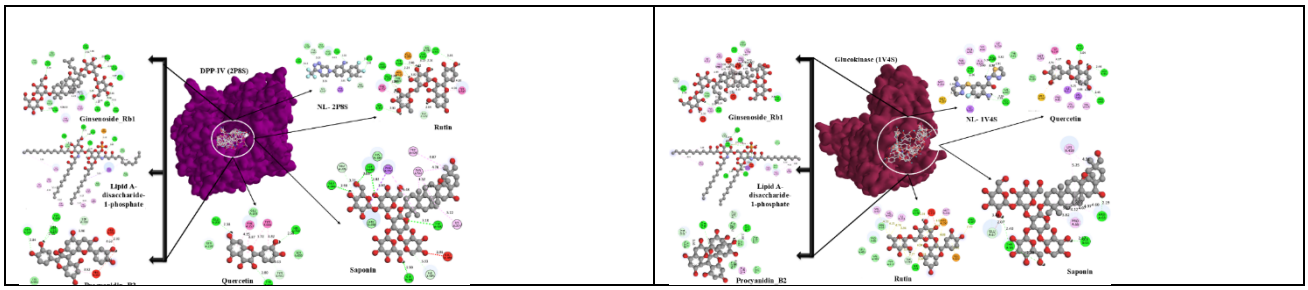

Figure 7. 2D and 3D representations of all potent derivatives, as well as all enzymes with their native ligands

CONCLUSION

This study thoroughly examined the Unani polyherbal formulation QZKH on its physicochemical, phytochemical, and pharmacological characteristics, validating its safety, quality, and effectiveness in diabetes treatment. Organoleptic and physicochemical evaluations revealed ideal moisture levels, almost neutral pH, and the lack of heavy metals or microbiological contamination, hence guaranteeing product stability and safety. Phytochemical analysis identified flavonoids, alkaloids, tannins, and saponins—bioactive compounds that confer antioxidant, hypoglycemic, and metabolic regulating effects. LC-HRMS profiling revealed significant components including rutin, quercetin, procyanidin B2, ginsenoside Rb1, and saponins, which jointly facilitate α-amylase and α-glucosidase inhibition, enhance insulin sensitivity, and provide β-cell protection. ADMET and molecular docking investigations corroborated these findings, demonstrating that substances such as quercetin, rutin, and procyanidin B2 had robust binding affinities with critical diabetes enzymes and advantageous pharmacokinetic features, equivalent to or exceeding those of native ligands. Furthermore, toxicity evaluations verified little cytotoxicity and favorable environmental safety profiles. The amalgamation of ancient Unani wisdom with contemporary analytical and computational methodologies scientifically validates the therapeutic effectiveness of QZKH as a safe and powerful antidiabetic formulation with multifaceted pharmacological capabilities.

.

REFERENCES

1. Petersmann A, Nauck M, Müller-Wieland D, Kerner W, Müller UA, Landgraf R, et al. Definition, classification and diagnostics of diabetes mellitus. J Lab Med. 2018;42(3):73–79.
2. Hossain MJ, Al-Mamun M, Islam MR. Diabetes mellitus, the fastest growing global public health concern: Early detection should be focused. Health Sci Rep. 2024;7(3):e2004.
3. Lestari L, Zulkarnain Z. Diabetes Melitus: Review etiologi, patofisiologi, gejala, penyebab, cara pemeriksaan, cara pengobatan dan cara pencegahan. Pros Sem Nas Biol. 2021;7(1):237–41.
4. Ojo OA, Ibrahim HS, Rotimi DE, Ogunlakin AD, Ojo AB. Diabetes mellitus: From molecular mechanism to pathophysiology and pharmacology. Med Novel Technol Devices. 2023;19:100247.
5. Siam NH, Snigdha NN, Tabasumma N, Parvin I. Diabetes Mellitus and Cardiovascular Disease: Exploring epidemiology, pathophysiology, and treatment strategies. Rev Cardiovasc Med. 2024;25(12):436.

6. Iheagwam FN, Iheagwam OT. Diabetes Mellitus: The pathophysiology as a canvas for management elucidation and strategies. Med Novel Technol Devices. 2025;100351.
7. Eqbal K, Alam MA, Quamri MA, Sofi G, Ahmad Bhat MD. Efficacy of Qurs-e-Gulnar in Ziabetus (type 2 diabetes mellitus): A single blind randomized controlled trial. J Complement Integr Med. 2021;18(1):147–53.
8. Hamiduddin M, Ali W, Jahangeer G, Al A. Unani formulations for management of diabetes: An overview. Int J Green Pharm. 2018;12(4):S769–83.
9. Khan SL, Bakshi V. LC-HRMS and in silico analysis of Ailanthus excels metabolites targeting EGFR triple mutation (L858R/T790M/C797S). Adv J Chem Sect A. 2026;9(2):292–311.
10. Zhong HA. ADMET properties: Overview and current topics. In: Drug Design: Principles and Applications. 2017. p.113–33.
11. Dong J, Wang NN, Yao ZJ, Zhang L, Cheng Y, Ouyang D, et al. ADMETlab: A platform for systematic ADMET evaluation based on a comprehensively collected ADMET database. J Cheminform. 2018;10(1):29.
12. Shastri MA, Gadhave R, Talath S, Wali AF, Hani U, Puri S, et al. In silico screening, synthesis, and in vitro enzyme assay of 1,2,3-oxadiazole-linked tetrahydropyrimidine-5-carboxylate derivatives as DPP-IV inhibitors for treatment of T2DM. Chem Methodol. 2024;8(11):800–19.
13. Suryawanshi RM, Shimpi RB, Muralidharan V, Nemade LS, Gurugubelli S, Baig S, et al. ADME, toxicity, molecular docking, molecular dynamics, glucokinase activation, DPP-IV, α-amylase, and α-glucosidase inhibition assays of mangiferin and friedelin for antidiabetic potential. Chem Biodivers. 2025;22(5):e202402738.
14. Vawhal PK, Jadhav SB, Kaushik S, Panigrahi KC, Nayak C, Urmee H, et al. Coumarin-based sulfonamide derivatives as potential DPP-IV inhibitors: Pre-ADME analysis, toxicity profile, computational analysis and in vitro enzyme assay. Molecules. 2023;28(3):1004.
15. Sarraf M, Sani AM, Atash MM. Physicochemical, organoleptic characteristics and image analysis of doughnut enriched with oleaster flour. J Food Process Preserv. 2017;41(4):e13021.
16. Pirzada AS, Khan H, Alam W, Darwish HW, Elhenawy AA, Kuznetsov A, Daglia M. Physicochemical properties, pharmacokinetic studies, DFT approach and antioxidant activity of nitro and chloro indolinone derivatives. Front Chem. 2024;12:1360719.
17. Siraj MB. Quality control and phytochemical validation of Saussurea lappa (Costus/Qust). Int J Green Pharm. 2020;14(1).
18. Sharma M, Abid R, Sajgotra M. Phytochemical screening and thin-layer chromatography of Ficus carica leaves extract. Pharm Biosci J. 2017:18–23.
19. Parvatikar PP, Madagi SB. Preliminary phytochemical analysis and biological screening of Indigofera hochestetteri. Pharma Innov J. 2018;7:503.
20. Ahmad N, Shakil A, Shinwari ZK, Ahmad I, Wahab A. Phytochemical study and antimicrobial activities of extracts and derived fractions from Berberis vulgaris L. and Stellaria media L. leaves. Pak J Bot. 2022;54(4):1517–21.
21. Sevindik M, Rasul A, Hussain G, Anwar H, Zahoor MK, Sarfraz I, et al. Determination of antioxidative, antimicrobial activity and heavy metal contents of Leucoagaricus leucothites. Pak J Pharm Sci. 2018;31(5):2163–8.
22. Sharma P, Rathore P, Choudhary Y, Tatwade Y, Joshi A. Anti-microbial activity of seed oils and protein estimation of seed content in Clitoria ternatea, Lagenaria siceraria and Ziziphus mauritiana. Braz J Sci. 2023;2(8):41–6.
23. Nurani LH, Kumalasari E, Zainab Z, Mursyidi A, Widyarini S, Rohman A. Determination of metal content, microbial contamination and dissolution assessment of ethanol extract of Pasak Bumi root. J Pharmaciana. 2017;7:295–304.
24. Luca SV, Minceva M, Gertsch J, Skalicka-Woźniak K. LC-HRMS/MS-based phytochemical profiling of Piper spices: Global association of piperamides with endocannabinoid system modulation. Food Res Int. 2021;141:110123.
25. Aryal B, Adhikari B, Aryal N, Bhattarai BR, Khadayat K, Parajuli N. LC-HRMS profiling and antidiabetic, antioxidant and antibacterial activities of Acacia catechu (Lf) Willd. Biomed Res Int. 2021;2021:7588711.
26. Kızıltaş H, Bingol Z, Goren AC, Pınar SM, Alwasel SH, Gülçin İ. LC-HRMS profiling of phytochemicals, antidiabetic, anticholinergic and antioxidant activities of ethanol extract of Astragalus brachycalyx Fischer.
27. Tamboli AS, Tayade SD. In-depth investigation of berberine and tropane through computational screening as DPP-IV inhibitors for treatment of T2DM. J Pharm Sci Comput Chem. 2025;1(1):1–1.
28. Khan A, Unnisa A, Sohel M, Date M, Panpaliya N, Saboo SG, et al. Investigation of phytoconstituents of Enicostemma littorale as potential glucokinase activators through molecular docking for treatment of T2DM. In Silico Pharmacol. 2021;10(1):1.
29. Joshi M, Pathan I, Sahu A, Raza A, Sahu Y, Khatoon

N. Computational chemistry in structure-based drug design: Tools, trends and transformations. J Pharm Sci Comput Chem. 2025;1(3):246–66.

30. Ahmed SA, Tabassum PS, Falak SA, Ahmad AV, Shaikh MS. Molecular docking and network pharmacology: Investigating Vitis vinifera phytoconstituents as multi-target agents against breast cancer. J Pharm Sci Comput Chem. 2025;1(2):116–34.
31. Hani U, Al-Qahtani E, Albeeshi F, Alshahrani S. Exploring the landscape of drug–target interactions: Molecular mechanisms, analytical approaches and case studies. J Pharm Sci Comput Chem. 2025;1:12–25.
32. Jadhav SS, Dighe PR. In vitro evaluation and molecular docking studies of novel pyrazoline derivatives as promising bioactive molecules. J Pharm Sci Comput Chem. 2025;1(3):190–209

.